A hybrid Galerkin atmospheric model

S.J. Thomas*, A. St-Cyr, R.D. Nair

National Center for Atmospheric Research, 1850 Table Mesa Drive, Boulder, CO 80305, USA

Abstract

The purpose of this paper is to explore a time-split hybrid Galerkin scheme for the atmospheric shallow water equations. A nonlinear variant of operator integration factor splitting is employed as the time-stepping scheme. The hyperbolic system representing slow modes is discretized using the discontinuous Galerkin method. An implicit second-order backward differentiation formula is applied to Coriolis and gravity wave terms. The implicit system is then discretized using a spectral element or continuous Galerkin method. The advantages of such an approach include improved mass and energy conservation properties. A TVD Runge-Kutta scheme is used for sub-stepping.

Keywords: Integration factor; High-order methods; Shallow water equations

1. Introduction

Semi-implicit time-stepping is often applied to the terms responsible for fast waves in atmospheric general circulation models to remove the time step restrictions associated with these waves. Both the phase and amplitude of the fastest gravity waves are distorted in such numerical models. Because these waves carry very little energy, this does not significantly impact the large-scale flow. In meteorology, the semi-implicit method was first introduced by Kwizak et al. [1]. Staniforth et al. [2] analyzed the stability of the second-order accurate Crank-Nicholson leapfrog (CNLF) semi-implicit scheme in the context of a finite element shallow water model.

The seminal work of Robert [3] led to a six-fold increase over the explicit time step for atmospheric general circulation models. To achieve such dramatic gains without recourse to a fully implicit integrator, a semi-Lagrangian treatment of advection was combined with a semi-implicit scheme for the stiff terms responsible for gravity waves. Initially, semi-implicit semi-Lagrangian time-stepping was applied to hyperbolic problems, discretized using low-order finite-differences and finite elements. The traditional semi-Lagrangian algorithm implemented in atmospheric models relies on backward trajectory integration and upstream interpolation [4]. A mass-conservative cell-integrated variant of the algorithm was recently developed by Nair et al.

[5]. A potentially lower cost alternative is the operator integrating factor splitting (OIFS) method of Maday et al. [6] which relies on Eulerian sub-stepping of the advection equation. In contrast with semi-Lagrangian advection, there are no dissipation or dispersion errors associated with upstream interpolation or trajectory integration and the scheme maintains the high-order accuracy of the discrete spatial operators.

A discontinuous Galerkin shallow water model employing a nodal basis and explicit time-stepping is described in Giraldo et al. [7]. Sherwin [8] demonstrated the advantages of a hybrid Galerkin approach in the context of the incompressible Navier-Stokes equations. Eskilsson et al. [9] describe a discontinuous Galerkin formulation of the shallow water equations using third-order TVD Runge-Kutta time-stepping. Here, we investigate a time-split scheme applied to the global shallow water equations in curvilinear coordinates on the cubed-sphere. A second-order backward differentiation formula (BDF-2) is combined with TVD-RK sub-stepping of a hyperbolic system. Because the incompressibility constraint has been removed, the fully nonlinear OIFS scheme of St-Cyr et al.[10] is employed. When compared to spectral elements, the hybrid scheme results in improved mass and energy conservation properties. For smooth solutions, there is no need to stabilize the time-stepping scheme with filters or limiters.

---

* Corresponding author. Tel.: +1 (303) 497 1841; Fax: +1 (303) 497 1286; E-mail: thomas@ucar.edu

2. Shallow water equations

The shallow water equations have been used as a vehicle for testing promising numerical methods for many years by the atmospheric modeling community. They contain the essential wave propagation mechanisms found in atmospheric general circulation models. These are the fast-moving gravity waves and nonlinear Rossby waves. The latter are important for correctly capturing nonlinear atmospheric dynamics. The governing equations of motion for the inviscid flow of a free surface are

$$\frac{\partial \mathbf{v}}{\partial t} + (f + \zeta)\,\mathbf{k} \times \mathbf{v} + \frac{1}{2}\nabla(\mathbf{v} \cdot \mathbf{v}) + \nabla\Phi = 0 \tag{1}$$

$$\frac{\partial \Phi}{\partial t} + (\mathbf{v} \cdot \nabla)\,\Phi + (\Phi_0 + \Phi)\nabla \cdot \mathbf{v} = 0 \tag{2}$$

h is the height above sea level, $\mathbf{v}$ is the horizontal velocity and $\Phi = gh$ the geopotential height. f is the Coriolis parameter and $\mathbf{k}$ a unit vector in the vertical direction. The geopotential height is decomposed into a perturbation about a constant base state, Φ_0. To exploit the potential of operator integration factor splitting for systems of time-dependent partial differential equations, St-Cyr et al.[10] show that a fully nonlinear form of the algorithm is more appropriate. Sub-stepping is applied to

$$\frac{\partial \tilde{\mathbf{v}}}{\partial s} + \tilde{\zeta}\,\mathbf{k} \times \tilde{\mathbf{v}} + \frac{1}{2}\nabla(\tilde{\mathbf{v}} \cdot \tilde{\mathbf{v}}) = 0 \tag{3}$$

$$\frac{\partial \Phi}{\partial s} + \nabla \cdot (\tilde{\Phi}\,\tilde{\mathbf{v}}) = 0 \tag{4}$$

with initial conditions $\tilde{\mathbf{v}}(\mathbf{x}, t^{n-q}) = \mathbf{v}(\mathbf{x}, t^{n-q})$, $\tilde{\Phi}(\mathbf{x}, t^{n-q}) = \Phi(\mathbf{x}, t^{n-q})$. The integration factor $Q_S^{t*}(t)$ is applied to the remaining de-coupled system of equations containing the Coriolis and linear gravity wave terms

$$\frac{d}{dt}Q_S^{t*}(t)\begin{bmatrix} \mathbf{v} \\ \Phi \end{bmatrix} = -Q_S^{t*}(t)\begin{bmatrix} f\,\mathbf{k} \times \mathbf{v} + \nabla\Phi \\ \Phi_0\nabla \cdot \mathbf{v} \end{bmatrix} \tag{5}$$

An accurate representation of fast-moving gravity waves is not required for large scale atmospheric dynamics and the corresponding terms can be treated implicitly. For an implicit second-order BDF-2 scheme, sub-stepping of the right-hand-side terms is not required because $Q_S^{t^n}(t^n) = I$. The resulting time discretization of Eq. (5) is given by

$$\mathbf{v}^n + \frac{2}{3}\Delta t\,\mathbf{N}\nabla\Phi^n = \frac{4}{3}\mathbf{N}\tilde{\mathbf{v}}^{n-1} - \frac{1}{3}\mathbf{N}\tilde{\mathbf{v}}^{n-2} \tag{6}$$

$$\Phi^n + \frac{2}{3}\Delta t\,\Phi_0\nabla \cdot \mathbf{v}^n = \frac{4}{3}\tilde{\Phi}^{n-1} - \frac{1}{3}\tilde{\Phi}^{n-2} \tag{7}$$

where

$$\mathbf{N} = \left(I + \frac{2}{3}\Delta t f\mathbf{M}\right)^{-1}, \quad \mathbf{M} = \begin{bmatrix} 0 & -1 \\ 1 & 0 \end{bmatrix} \tag{8}$$

The values of the fields $\tilde{\mathbf{v}}$ and $\tilde{\Phi}$ at time levels $n - 1$ and $n - 2$ are computed by sub-stepping Eqs. (3) and (4) on the intervals $[t^{n-1}, t^n]$ and $[t^{n-2}, t^n]$. An implicit equation for Φ^n is obtained after space discretization and application of block Gaussian elimination, resulting in a modified Helmholtz problem. The coefficient matrix of this linear system of equations is non-symmetric due to the implicit treatment of the Coriolis terms and is solved using an iterative conjugate-gradient squared (CGS) algorithm.

For spectral elements, the linear advection operator is skew-symmetric with purely imaginary eigenvalues. Therefore, an efficient time integration scheme for sub-stepping should have a stability region that includes a portion of the imaginary axis. Numerical quadrature can shift some of these eigenvalues into the right-half plane and a filter is required to stabilize the time-stepping scheme [11]. A discontinuous Galerkin space discretization, in combination with a total variation diminishing (TVD) Runge-Kutta integrator, preserves strong stability [12]. For smooth solutions, a filter or limiter is not required to stabilize the time-stepping scheme. In the next section we describe the cube-sphere computational domain, discontinuous Galerkin approximations and TVD-RK sub-stepping.

3. High-order Galerkin approximations

The flux form shallow-water equations in curvilinear coordinates are described in Sadourny [13]. Let $\mathbf{a}_1$ and $\mathbf{a}_2$ be the covariant base vectors of the transformation between inscribed cube and spherical surface. The metric tensor of the transformation is defined as $G_{ij} \equiv \mathbf{a}_i \cdot \mathbf{a}_j$. Covariant and contravariant vectors are related through the metric tensor by $u_i = G_{ij}u^j$, $u^i = G^{ij}u_j$, where $G^{ij} = (G_{ij})^{-1}$ and $G = \det(G_{ij})$. The six local coordinate systems (x^1, x^2) are based on equiangular central projection, $-\pi/4 \le x^1, x^2 \le \pi/4$. The metric tensor for all six faces of the cube is

$$G_{ij} = \frac{1}{r^4 \cos^2 x^1 \cos^2 x^2}\begin{bmatrix} 1 + \tan^2 x^1 & -\tan x^1 \tan x^2 \\ -\tan x^1 \tan x^2 & 1 + \tan^2 x^2 \end{bmatrix} \tag{9}$$

where $r = (1 + \tan^2 x^1 + \tan^2 x^2)^{1/2}$ and $\sqrt{G} = 1/r^3 \cos^2 x^1 \cos^2 x^2$.

In curvilinear coordinates, the time-split hyperbolic system (3)–(4) becomes

$$\frac{\partial u_1}{\partial t} + \frac{\partial}{\partial x^1}E = -\sqrt{G}u^2(f + \zeta) \tag{10}$$

$$\frac{\partial u_2}{\partial t} + \frac{\partial}{\partial x^2} E = -\sqrt{G} u^1 (f + \zeta) \tag{11}$$

$$\frac{\partial}{\partial t}(\sqrt{G}\Phi) + \frac{\partial}{\partial x^1}(\sqrt{G}u^1\Phi) + \frac{\partial}{\partial x^2}(\sqrt{G}u^2\Phi) = 0 \tag{12}$$

where

$$E = \frac{1}{2}(u_1 u^1 + u_2 u^2), \quad \zeta = \frac{1}{\sqrt{G}}\left[\frac{\partial u_2}{\partial x^1} - \frac{\partial u_1}{\partial x^2}\right]$$

The hyperbolic system (10)–(12) may be expressed in the general flux form,

$$\frac{\partial}{\partial t}\mathbf{U} + \frac{\partial}{\partial x^1}\mathbf{F}_1 + (\mathbf{U}) + \frac{\partial}{\partial x^2}\mathbf{F}_2(\mathbf{U}) = \mathbf{S}(\mathbf{U}) \tag{13}$$

Consider a scalar component of Eq. (13)

$$\frac{\partial U}{\partial t} + \nabla \cdot \mathcal{F}(U) = S(U), \quad \text{in} \quad \Omega \times (0,T) \tag{14}$$

The computational domain Ω is partitioned into non-overlapping elements Ω_k. An approximate solution U_h belongs to the finite dimensional space $\mathcal{V}_h(\Omega)$. Multiplication of Eq. (14) by a test function $\varphi_h \in \mathcal{V}_h$ and integration over the element Ω_k results in a weak Galerkin formulation of the problem.

$$\frac{\partial}{\partial t}\int_{\Omega_k}\varphi_h U_h d\Omega = \int_{\Omega_k}\varphi_h S(U_h)\, d\Omega + \int_{\Omega_k}\mathcal{F}(U_h)\cdot\nabla\varphi_h d\Omega$$
$$- \int_{\partial\Omega_k}\varphi_h \mathcal{F}\cdot\hat{n}\, ds \tag{15}$$

For a discontinuous Galerkin approximation, a nodal basis for $\mathcal{V}_h$ is employed, consisting of the Legendre cardinal functions. The solutions U_h are expanded in terms of tensor-product basis functions on a Gauss-Lobatto grid.

The flux function $\mathcal{F}(U_h)\cdot\hat{n}$ is approximated by a Lax-Friedrichs numerical flux

$$\hat{\mathcal{F}}(U_h^-, U_h^+) = \frac{1}{2}\left[(\mathcal{F}(U_h^-) + \mathcal{F}(U_h^+))\cdot\hat{n} - \alpha(U_h^+ - U_h^-)\right] \tag{16}$$

Boundary integrals are computed using higher-order Gaussian quadrature. α is the upper bound for the absolute value of eigenvalues of the flux Jacobian $\mathcal{F}'(U)$ in the direction $\hat{n}$. For the cubed-sphere, Nair et al. [14] derived

$$\alpha^1 = \max\left(|u^1| + \sqrt{\Phi G^{11}}\right), \quad \alpha^2 = \max\left(|u^2| + \sqrt{\Phi G^{22}}\right) \tag{17}$$

Equations (10–12) can be written in the semi-discrete form

$$\frac{d}{dt}\mathbf{U} = \mathbf{L}(\mathbf{U}) \quad \text{in} \quad (0,T) \tag{18}$$

A third-order total variation diminishing Runge-Kutta (TVD-RK) scheme is applied to sub-step the above system of ordinary differential equations [15]. The implicit system (6)–(7) is discretized using the $\mathbb{P}_N - \mathbb{P}_{N-2}$ spectral element method.

4. Numerical experiments

Our numerical experiments are based on the shallow water test suite of Williamson et al. [16]. Test case 5 is a zonal flow impinging on an isolated mountain. The center of the mountain is located at $(3\pi/2, \pi/6)$ with height $h_s = 2000\,(1 - r/R)$ meters, where $R = \pi/9$ and $r^2 = \min[R^2, (\lambda - 3\pi/2)^2 + (\theta - \pi/6)^2]$. Initial wind and height fields are

$$u = u_0(\cos\alpha_0\cos\theta + \sin\alpha_0\cos\lambda\sin\theta)$$
$$v = -u_0\sin\alpha_0\sin\lambda$$
$$g\,h = g\,h_0 - \frac{u_0}{2}(2a\,\Omega + u_0)$$
$$(\sin\theta\cos\alpha_0 - \cos\lambda\cos\theta\sin\alpha_0)^2$$

where a is the earth's radius, Ω the rotation rate, $\alpha_0 = 0$, $gh_0 = 5960$ m^2/s^2 and $u_0 = 20$ m/s.

The geopotential height field after 15 days of integration is plotted in Fig. 1. The solution is smooth and does not exhibit spurious oscillations. Conservation of integral invariants is monitored with the normalized integral defined in Williamson et al.[16],

$$\bar{\psi}(t) = \frac{I_g[\psi(\lambda,\theta,t)] - I_g[\psi(\lambda,\theta,0)]}{I_g[\psi(\lambda,\theta,0)]} \tag{19}$$

Normalized discrete mass, energy and potential enstrophy are plotted as a function of time in Fig. 2. The top panel shows that mass lost during the integration is far less than observed in Thomas et al. [17] and St-Cyr et al. [10] for the same test using a spectral element discretization. There is a gradual degradation in total energy, and total potential enstrophy remains nearly constant.

5. Conclusions

Despite the more restrictive time step associated with the third-order TVD-RK scheme, the efficiency of the time-split hybrid Galerkin scheme is comparable to the pure spectral element discretization. This is partially due to the fact that the computation time is dominated by an increasing number of CGS solver iterations with the time step length. Improved preconditioning strategies
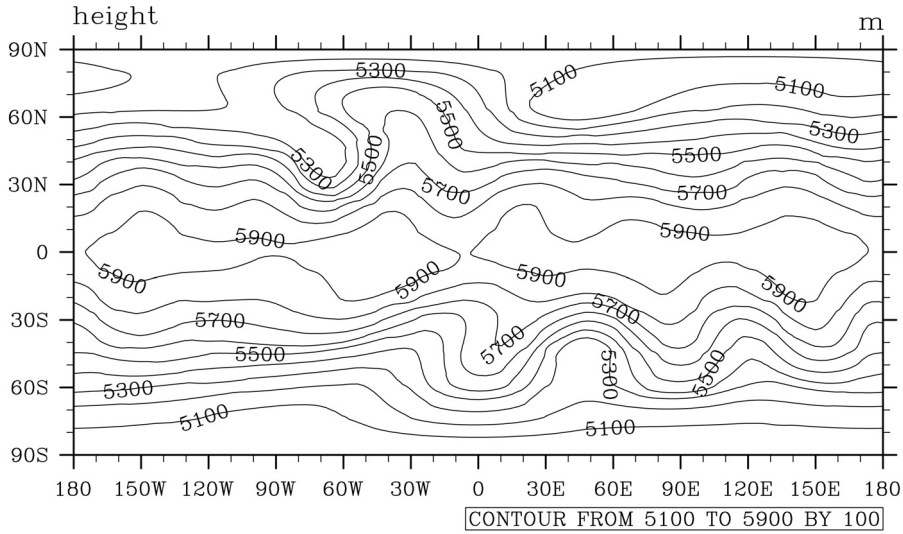
Fig. 1. Shallow water test case 5: flow impinging on a mountain. Geopotential height field h at fifteen days produced by hybrid scheme. 150 spectral elements, 8×8 Gauss-Legendre Lobatto points per element.
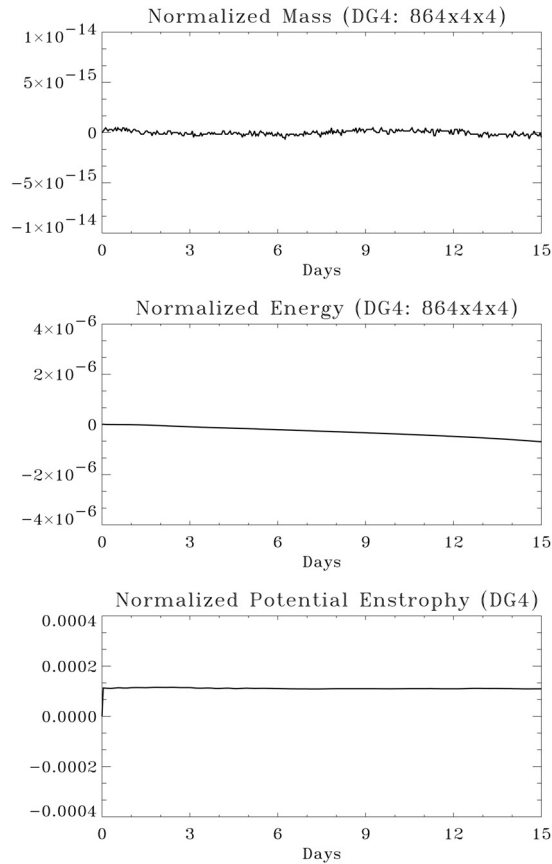
Fig. 2. Time traces of normalized integral invariants for SW test case 5. Top panel is total mass, central panel total energy and the bottom panel is potential enstrophy. 4×4 Gauss-Legendre Lobatto points per element. 864 elements.

would no doubt have an impact on the overall efficiency. For parallel computation, a clear advantage of the hybrid Galerkin scheme is the reduced communication overhead. In addition, filters or limiters are not required to stabilize the time-stepping scheme for smooth solutions. Although the proposed hybrid scheme is not strictly conservative, the mass loss is significantly less than in the case of a spectral element model.

References

[1] Kwizak M, Robert AJ. A semi-implicit scheme for grid point atmospheric models of the primitive equations. Mon Weather Rev 1971;99:32–36.

[2] Staniforth AN, Mitchell HJ. A semi-implicit finite-element barotropic model. Mon Weather Rev 1977;105:154–169.

[3] Robert AJ. A stable numerical integration scheme for the primitive meteorological equations. Atmos Ocean 1981;19:35–46.

[4] Staniforth A, Coté J. Semi-Lagrangian integration schemes for atmospheric models – a review. Mon Weather Rev 1991;119:2206–2223.

[5] Nair RD, Machenhauer B. The mass-conservative cell integrated semi-Lagrangian advection scheme over the sphere. Mon Weather Rev 2002;130:649–667.

[6] Maday Y, Patera AT, Ronquist EM. An operator-integration-factor splitting method for time-dependent problems: application to incompressible fluid flow. J Sci Comput 1990;5:263–292.

[7] Giraldo FX, Hesthaven JS, Warburton T. Nodal high-order discontinuous Galerkin methods for spherical shallow water equations. J Comput Phys 2003;181:499–525.

[8] Sherwin SJ. A sub-stepping Navier-Stokes splitting scheme for spectral/hp element discretisations. In: Parallel Computational Fluid Dynamics – New Frontiers and Multi-disciplinary Applications, K. Matsuno, A. Ecer, J. Periaux, N. Satofuka, editors, and P. Fox (assistant editor). Elsevier: 2003.

[9] Eskilsson C, Sherwin SJ. Discontinuous Galerkin spectral/hp element modelling of dispersive shallow water systems. J Sci Comp 2005;22:279–298.

[10] St-Cyr A, Thomas SJ. Nonlinear operator integration factor splitting for the shallow water equations. Appl Numer Math 2005;52:429–448.

[11] Fischer PF, Mullen JS. Filter-based stabilization of spectral element methods. Comptes Rendus de l'Académie des Sciences Paris, Série I: Analyse numérique 2001;332:265–270.

[12] Gottlieb S, Shu CW, Tadmor E. Strong stability preserving high-order time discretization methods. SIAM Review 2001;43:89–112.

[13] Sadourny R. Conservative finite-difference approximations of the primitive equations on quasi-uniform spherical grids. Mon Weather Rev 1972;100:136–144.

[14] Nair RD, Thomas SJ, Loft RD. A discontinuous Galerkin global shallow water model. Mon. Weather Rev 2005 (to appear).

[15] Cockburn B, Shu CW. The Runge-Kutta discontinuous Galerkin finite-element method for conservation laws V: multi-dimensional systems. J Comput Phys 1998;141:199–224.

[16] Williamson DL, Drake JB, Hack JJ, Jakob R, Swarztrauber PN. A standard test set for numerical approximations to the shallow water equations in spherical geometry. J Comput Phys 1992;102:211–224.

[17] Thomas SJ, Loft RD. Semi-implicit spectral element atmospheric model. J Sci Comput 2002;17:339–350.